Nanoscale Shear Deformation Mechanisms of Opposing Cartilage Aggrecan Macromolecules

Lin Han,* Delphine Dean,† Pan Mao,‡ Christine Ortiz,* and Alan J. Grodzinsky†‡§
*Departments of Materials Science and Engineering; †Electrical Engineering and Computer Science and ‡Mechanical Engineering; and §Biological Engineering, Massachusetts Institute of Technology, Cambridge, Massachusetts

ABSTRACT The nanoscale shear deformation behavior of two opposing end-grafted aggrecan layers was studied in aqueous solutions using atomic force microscopy, and was observed to depend markedly on bath ionic strength, the presence of calcium ions, and the applied lateral displacement rate. These results provide molecular-level insights into the contribution of aggrecan deformation mechanisms to cartilage tissue-level material properties.

Received for publication 31 May 2007 and in final form 20 June 2007.

Address reprint requests and inquiries to A. J. Grodzinsky, Tel.: 617-253-4969; E-mail: alg@mit.edu.

Aggrecan, the most abundant proteoglycan in cartilage comprising 30–35% of tissue dry weight, has a densely-packed array of highly negatively charged chondroitin sulfate glycosaminoglycan chains along its core protein (1) and is critical to cartilage mechanical function (2). Recently, we quantified shear interactions within a chemically end-grafted aggrecan layer using neutral nanosized and microsized (colloidal) probe tips via lateral force microscopy (3). At near physiological ionic strength (IS = 0.1 M, pH ~ 5.6), linearity was observed between lateral and normal forces applied to the aggrecan (linearity ratio $\mu = 0.06 \pm 0.01$ at 60 μm/s lateral displacement rate). Both electrostatic and nonelectrostatic contributions to shear interactions were identified, and μ increased nonlinearly with lateral displacement rate to 0.09 ± 0.01 at 100 μm/s. These results suggested the presence of visco/poroelastic rate processes within the aggrecan layer at the nanoscale (3). Here, we report lateral interactions between two opposing end-attached aggrecan layers, a configuration that more closely mimics aggrecan interactions during shear deformation of intact cartilage in vivo. In addition, we demonstrate the effects of Ca^{2+} at physiological concentration on these shear interactions, along with effects of varying bath IS and displacement rate.

Hexagonal-patterned substrates with end-anchored bovine fetal epiphyseal aggrecan inside 10-μm-sided hexagons, and neutral hydroxyl-terminated self-assembled monolayers outside the hexagons (OH-SAM, height ~1 nm, $HS(CH_2)_{11}OH$; Aldrich, St. Louis, MO), were prepared via microcontact printing, as described previously (4). Aggrecan packing density was within the physiological range (one aggrecan per ~25 nm × 25 nm, or ~24 ± 5 mg/mL at 0.1 M IS (4)). Aggrecan functionalized probe tips were prepared in a similar fashion by 48 h incubation of gold-coated colloidal probe tips (end radius $R_{tip} \sim 2.5$ μm, nominal spring constant $k \sim 0.12$ N/m; Bioforce Nanosciences, Ames, IA) in 100 μL of the 1 mg/mL thiol-functionalized aggrecan solution (5). By these methods, ~10^3 aggrecan molecules in each layer could interact simultaneously. Normal and lateral forces were measured and calibrated using a MultiMode Nanoscope IV atomic force microscope (AFM) with a PicoForce piezo (Veeco, Santa Barbara, CA) via lateral force microscopy (3). The total height of the two opposing aggrecan layers (H in Fig. 1 *a*) was measured by AFM imaging of microcontact printed surfaces (5). H was converted to normal strain ε_n by normalization to the height measured by AFM imaging at negligible normal force (3). The measured aggrecan layer height and lateral force were independent of loading history, suggesting that there was negligible shear-induced irreversible damage or conformational changes in the end-attached aggrecan layers.

Upon shear deformation (Fig. 1 *a*), the measured lateral force varied linearly with applied normal force (Fig. 1 *b*); at a given normal force, the lateral force increased with increasing IS. Lateral force increased nonlinearly with decreasing aggrecan height (Fig. 1 *c*) and increasing normal strain (Fig. 1 *d*) at all IS. At constant height (Fig. 1 *c*) the lateral force decreased with increasing IS, but the lateral force was less sensitive to changes in IS at constant strain (Fig. 1 *d*). These trends for two opposing aggrecan layers were similar to those observed with a single layer sheared by a neutral hard-wall OH-SAM probe tip (3), except for those of Fig. 1 *d*, where differences with IS were more pronounced in the single layer. Differences in lateral deformability as a function of IS at constant aggrecan height and strain (Fig. 1, *c* and *d*) suggest the presence of electrostatic interactions. Nonelectrostatic interactions (e.g., excluded volume, steric, entropic, van der Waals, and possible molecular interpenetration and/or entanglement) were evident in the two-layer configuration, as demonstrated by marked differences in lateral force with changes in IS when calculated at constant values of the ratio

Editor: Dagmar Ringe.

doi: 10.1529/biophysj.107.114025

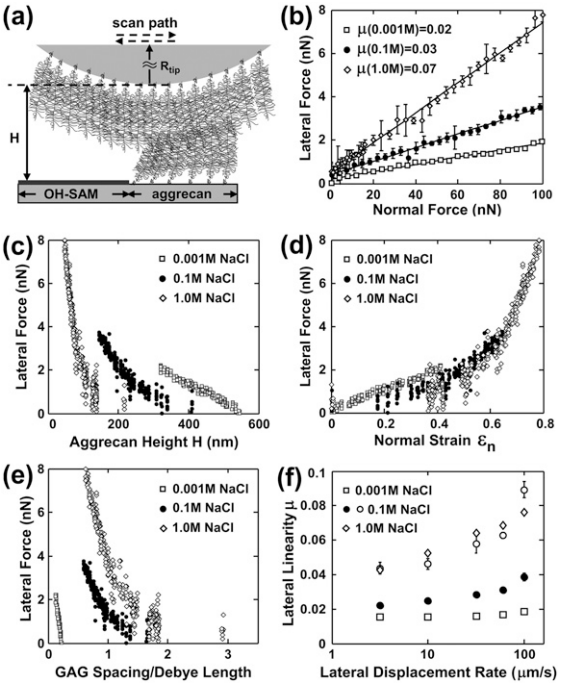

FIGURE 1 (*a*) **Lateral motion of two opposing aggrecan layers using an aggrecan functionalized probe tip ($R_{tip} \sim 2.5$ μm) on an aggrecan-OH-SAM micropatterned sample. (*b*) Lateral versus applied normal force (mean ± SD, $n = 8$ different locations), 95% confidence interval of $\mu < \pm 0.01$, estimated via least-squares linear regression (LSLR), $R^2 > 0.92$ for all IS. (*c*) Lateral force versus total height H of two aggrecan layers. (*d*) Lateral force versus normal strain ε_n. (*e*) Lateral force versus estimated ratio of GAG spacing to Debye length. Each data point in panels *c*–*e* represents one lateral scan. (*f*) Lateral proportionality μ versus lateral tip displacement rate (mean ± 95% confidence interval at $n = 8$ different locations via LSLR, $R^2 > 0.88$ for all data). Open circles denote μ measured via an OH-SAM tip at 0.1 M IS, adapted from Han et al. (3) ($R^2 > 0.81$ for all data). Effects of displacement rate (one-way ANOVA, $p < 0.0001$ at all IS) and IS (two-way ANOVA, $p < 0.0001$) are significant. Experiments performed in NaCl, pH ~ 5.6.**

of GAG spacing to electrical Debye length (Fig. 1 *e*), which were also observed in the single-layer studies (3).

Interestingly, there were important differences between the two-layer system studied here and the single-layer system studied previously (3). In general, the lateral force between the opposing aggrecan layers (Fig. 1, *b*–*e*) was observed to be ~20–50% less than that in the single layer (3) under the same experimental conditions, i.e., normal force, normal strain, and IS, similar to the trend observed for normal compressive loading (5). The increased lateral compliance of two opposing layers compared to a single layer is attributed to a change in the molecular mechanisms of deformation (5). One possibility is interpenetration of aggrecan layers, which is expected to increase the degree of molecular mobility compared to the single layer system in which lateral deformation is more restricted by the use of a hard-wall probe tip. Another possibility is that the local z-dependent charge density distribution for opposing layers would be altered compared to a single layer system with the highest charge density in the region of interpenetration. Together, these effects could result in less resistance to shear deformation of each aggrecan macromolecule. At the same normal strain ε_n (Fig. 1 *d*), lateral forces at different IS did not vary as markedly as those of the single layer (3), further suggesting that conformational mobility is an important determinant of lateral resistance. Lateral force increased significantly with lateral displacement rate at 0.001–1.0 M IS (Fig. 1 *f*). Rate-dependent mechanisms may include viscoelastic processes such as molecular friction between chain segments, molecular reorientation/reconfiguration, and possible interpenetration and entanglement of adjacent aggrecan. Poroelastic rate processes could occur, related to local fluid flow within and through the aggrecan molecules. With increasing IS, nonelectrostatic components become relatively more important, consistent with our observation that the rate dependence was more pronounced at higher IS. In contrast to Fig. 1 *f*, the lateral linearity coefficient for a single layer of aggrecan at 0.001 M IS did not show rate dependence (3). This difference is consistent with the possibility of interpenetration of the two opposing aggrecan layers where nonelectrostatic interactions would be important even at low IS. Adhesion-related friction mechanisms (6) appear to contribute minimally to shear resistance, as adhesion between the two opposing layers became important only when the layers were held in contact statically for sufficient time to equilibrate. We found previously that rapid detachment of the two layers resulted in negligible adhesion compared to the measured shear force (7). Here, no surface equilibration time was allowed during scanning and, as a result, adhesion between opposing layers was small.

We then studied the effect of physiologically relevant calcium concentration on the shear behavior of opposing aggrecan layers ($[Ca^{2+}]$ ~2–4 mM in synovial fluid (2)). Addition of divalent ions can also decrease electrostatic interactions in biological polyelectrolyte systems (8). The experiments of Fig. 2 were performed using a buffer of NaCl + $CaCl_2$: $[Cl^-]$ was maintained at 0.15 M and as $CaCl_2$ was added, NaCl was decreased accordingly. Increasing $[Ca^{2+}]$ from ~0 to 0.2 to 2 mM caused an increase in μ (Fig. 2 *a*); however, further increases in $[Ca^{2+}]$ from 2 to 75 mM did not change μ. The presence of Ca^{2+} is thought to enhance electrostatic screening by its valence and preferential distribution closer to GAGs than monovalent ions (9). Thus, the increase in μ with initial addition of Ca^{2+} (Fig. 2 *a*) is consistent with the trend seen with increasing [NaCl] in Fig. 1 *b*. In addition, however, Ca^{2+} (but not Na^+) can simultaneously neutralize negative charge groups by binding to both the carboxyl and sulfate moieties along the GAG chains within each of the aggrecan layers (10,11). Together, the screening and binding effects of Ca^{2+} can both lead to compaction of the two aggrecan layers, as seen in the decreased height at any given normal force (Fig. 2 *b*). This decreased height is equivalent to a decrease in the compressive stiffness of the combined opposing layers.

Interestingly, at a given height, aggrecan shear resistance was approximately the same at any $[Ca^{2+}]$ in the 0.2–75 mM

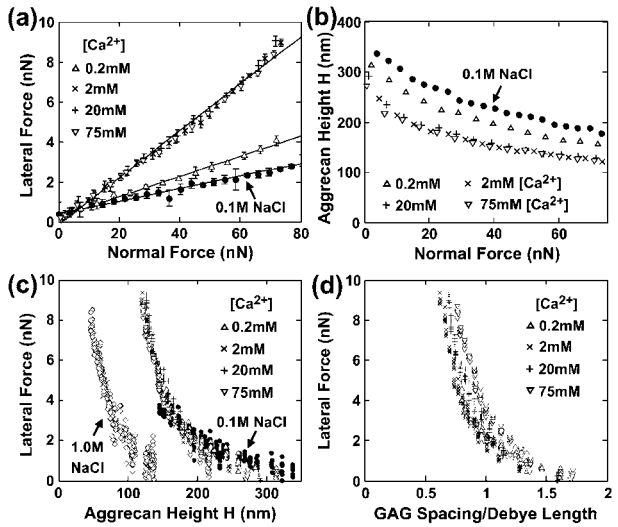

FIGURE 2 (*a*) Lateral versus applied normal force (mean ± SD, $n = 8$ different locations), $\mu = 0.05$ at 0.2 mM [Ca^{2+}] and 0.12 at 2–75 mM [Ca^{2+}], 95% confidence interval of $\mu < \pm 0.01$ via LSLR, $R^2 > 0.97$ for all [Ca^{2+}]. (*b*) Aggrecan total height *H* versus applied normal force ($n = 8$, mean ± SD < data size). (*c*) Lateral force versus height *H*. (*d*) Lateral force versus estimated ratio of GAG spacing to Debye length. In panels *c* and *d*, each data point represents one lateral scan. Experiments performed in NaCl + $CaCl_2$ solutions with [Cl^-] = 0.15 M, varying [Ca^{2+}] and [Na^+]; pH ~ 5.6. Data at 0.1 M NaCl in panel *b* is adapted from Dean et al. (5), for comparison.

range, though >1 M NaCl (Fig. 2 *c*). These data are replotted as a function of the ratio of GAG spacing to Debye length, as calculated for multivalent electrolyte solutions (Fig. 2 *d*) (9); again, lateral force appeared insensitive to added [Ca^{2+}] in the 0.2–75 mM range. Electrostatic double-layer repulsive interactions are similar at a constant value of this ratio under certain limiting conditions (3,9). Since increased screening would decrease long-range electrostatic contributions to shear resistance at constant height and constant GAG spacing/Debye length ratio (Fig. 2, *c* and *d*), the nonspecific screening effects associated with Ca^{2+} appear less important. Binding effects appear to saturate at [Ca^{2+}] ~2 mM (Fig. 2, *a* and *b*), consistent with the reported values of binding constants of Ca^{2+} to GAGs (12,13). Taken together, binding of Ca^{2+} to GAGs affects both aggrecan compressive and shear mechanical properties, consistent with the known effects of Ca^{2+} on cartilage tissue mechanics (8,12). Adhesive interactions due to Ca^{2+}-bridging between the two opposing aggrecan layers had minimal effect on aggrecan shear in this study, since the constant displacement rate does not allow the surface equilibration times (approximately seconds) necessary for adhesions between aggrecan to occur (7).

In vivo, up to ~100 aggrecan molecules are end-attached to hyaluronan filaments forming supramolecular aggregates enmeshed within a three-dimensional collagen network (1,2). Deformation and interactions between adjacent aggrecan occur within native cartilage as the tissue deforms during joint loading. While the two-dimensional end-attached aggrecan layer configuration used here is not identical to that within cartilage, our use of an aggrecan packing density within the physiological range (2) enables this system to replicate certain features of bulk tissue deformation, providing molecular-level insights into cartilage material properties. For example, joint-loading results in a combination of cartilage compression and shear, and their simultaneous effects on densely packed aggrecan can be studied with the present system (Figs. 1 and 2). Importantly, our nanoscale shear studies of opposing aggrecan layers demonstrate molecular-level rate and Ca^{2+}-dependent properties which are consistent with macroscopic poro-viscoelastic tissue properties (8,13), suggesting their importance to biomechanical functions.

ACKNOWLEDGMENTS

We thank the Massachusetts Institute of Technology's Institute for Soldier Nanotechnologies funded by U.S. Army Research Office for AFM use.

Supported by National Science Foundation-Nanoscale Interdisciplinary Research Teams grant No. 0403903, National Institutes of Health grant No. AR45779, and a Whitaker Foundation Fellowship (D.D.).

REFERENCES and FOOTNOTES

1. Hardingham, T. E., and A. J. Fosang. 1992. Proteoglycans: many forms and many functions. *FASEB J.* 6:861–870.
2. Maroudas, A. 1979. Physicochemical properties of articular cartilage. *In* Adult Articular Cartilage. M. A. R. Freeman, editor. Pitman Medical, London. 215–290.
3. Han, L., D. Dean, C. Ortiz, and A. J. Grodzinsky. 2007. Lateral nanomechanics of cartilage aggrecan macromolecules. *Biophys. J.* 92:1384–1398.
4. Dean, D., L. Han, C. Ortiz, and A. J. Grodzinsky. 2005. Nanoscale conformation and compressibility of cartilage aggrecan using microcontact printing and atomic force microscopy. *Macromolecules.* 38:4047–4049.
5. Dean, D., L. Han, A. J. Grodzinsky, and C. Ortiz. 2006. Compressive nanomechanics of opposing aggrecan macromolecules. *J. Biomech.* 39: 2555–2565.
6. Tomlinson, G. A. 1929. The molecular theory of friction. *Philos. Mag.* 7:905–916.
7. Han, L., D. Dean, L. A. Daher, A. J. Grodzinsky, and C. Ortiz. 2006. Biomolecular adhesion between opposing cartilage aggrecan macromolecules. 52nd Orthopedic Research Society, Chicago, IL. 361.
8. Grodzinsky, A. J., V. Roth, E. Myers, W. D. Grossman, and V. C. Mow. 1981. The significance of electromechanical and osmotic forces in the nonequilibrium swelling behavior of articular cartilage in tension. *J. Biomech. Eng. Trans. ASME.* 103:221–231.
9. Parker, K. H., C. P. Winlove, and A. Maroudas. 1988. The theoretical distributions and diffusivities of small ions in chondroitin sulphate and hyaluronate. *Biophys. Chem.* 32:271–282.
10. MacGregor, E. A., and J. M. Bowness. 1971. Interaction of proteoglycans and chondroitin sulfates with calcium or phosphate ions. *Can. J. Biochem.* 49:417–425.
11. Hunter, G. K., K. S. Wong, and J. J. Kim. 1988. Binding of calcium to glycosaminoglycans: an equilibrium dialysis study. *Arch. Biochem. Biophys.* 260:161–167.
12. Ehrlich, S., N. Wolff, R. Schneiderman, A. Maroudas, K. H. Parker, and C. P. Winlove. 1998. The osmotic pressure of chondroitin sulphate solutions. *Biorheology.* 35:383–397.
13. Setton, L. A., W. B. Zhu, and V. C. Mow. 1993. The biphasic poroviscoelastic behavior of articular cartilage: role of the surface zone in governing the compressive behavior. *J. Biomech.* 26:581–592.